Research Article

Shouliang Sun, Tao Zhang*, Yongfei Li, Shuwang Chen, and Qiushi Sun

Effects of igneous intrusions on source rock in the early diagenetic stage: A case study on Beipiao Formation in Jinyang Basin, Northeast China

https://doi.org/10.1515/geo-2020-0150
received May 14, 2020; accepted August 13, 2020

Abstract: Mesozoic intrusive bodies play an important role in the temperature history and hydrocarbon maturation of the Jinyang Basin in northeastern China. The Beipiao Formation, which is the main source rock in Jinyang Basin, was intruded by numerous igneous bodies and dykes in many areas. The effects of igneous intrusive bodies on thermal evolution and hydrocarbon generation and migration in the Beipiao Formation were investigated. A series of samples from the outcrop near the intrusive body were analyzed for vitrinite reflectance (R_0%) and other organic geochemical parameters to evaluate the lateral extension of the thermal aureole. The R_0 values of the samples increase from a background value of ~0.9% at a distance above 200 m from the intrusive body to more than 2.0% at the vicinity of the contact zone. The width of the altered zone is equal to the thickness of the intrusive body outcropped in the field. Organic geochemical proxies also indicate the intrusive body plays a positive and beneficial role in the formation of regional oil and gas resources. Due to the influence of the anomalous heat from the intrusive body, the hydrocarbon conversion rate of the source rocks of the Beipiao Formation was significantly improved. The accumulation properties and the storage capacity of the shales also greatly improved due to the intrusive body as indicated by the free hydrocarbon migration in the shales. This new understanding not only provides a reliable scientific basis for the accurate assessment of oil and gas genesis and resources in the Jinyang Basin but also provides guidance and reference for oil and gas exploration in the similar type of basin.

Key words: Jinyang Basin, igneous intrusions, anomalous heat, Beipiao formation, thermal evolution of source rocks

1 Introduction

Igneous intrusions are common in many sedimentary basins and had been much talked about for their significance effect on organic rich source rocks [1–11]. It has been clear that igneous intrusions can not only alter the physical but also the chemical characteristics of organic rick host rocks in many areas [12–22]. Numerous studies, both experimental and numerical, have reported the interactions between a petroleum system and intrusive bodies, especially igneous intrusions in coal measures, with a particular emphasis on the thermal effect of dykes on organic rich host rocks [1,9,23–25]. What's more, igneous intrusions can generate large volume of gas to form gas reservoirs or erupt into the atmosphere and can even trigger climate changes [1,26–28]. Many of the basins with large volume of igneous intrusions are petroliferous and targeted for hydrocarbon exploration and production. In Norway, the offshore Vøring and Møre basins intruded by extensive sill complexes in the Paleocene–Eocene are currently being targeted for their hydrocarbon potential [26]. The Karoo Basin of south Africa, lower Jurassic sills and dykes are present throughout the Karoo sedimentary sequence and have attracted strong interest for both conventional and unconventional oil and gas potential [29,30]. One of the main topics of these studies is to determine the thickness of thermal alteration aureole. The thickness of the intrusive body, host rock conductivity, porosity, permeability, and the amount of pore fluid involved are considered the main factors in determining the width of the altered zone [1,4,8,18,24,31,32]. Although the thermal effects of igneous intrusions have been discussed in numerous studies, few studies talked about its effects on hydrocarbon generation and expulsion in organic rich host

* **Corresponding author: Tao Zhang,** Shenyang Center of China Geological Survey, Shenyang, 110034, China; State Key Laboratory of Organic Geochemistry, Guangzhou Institute of Geochemistry, Chinese Academy of Sciences, Guangzhou, 510640, China, e-mail: ztao_89@foxmail.com
Yongfei Li, Shuwang Chen, Qiushi Sun: Shenyang Center of China Geological Survey, Shenyang, 110034, China
Shouliang Sun: Shenyang Center of China Geological Survey, Shenyang, 110034, China, e-mail: sunsolar@qq.com

rocks, especially in the early diagenetic stage. Based on the study of sills that are emplaced as clusters, it had been concluded that sills intruding with a time interval will show a positive effect on the thermal maturation of source rocks [1,11]. Still, additional works should be done for igneous intrusions that are emplaced at different time, especially in the early period of formation of the host rocks.

Jurassic volcanic activities were widespread and extensive in northeastern China. The magmatic activities were not restricted to now the mountainous areas, but also were widely found in Mesozoic sedimentary fault rift basins, especially in the early bottom sequence of the fault depressions. Most of the fault rift sedimentary basins were formed in the late stage of magmatism with some exceptions that formed during the intermittent period of volcanic activities [33].

The Jinyang Basin, located on the southern peripheral area of the Songliao Basin, is a typical volcanic-sedimentary basin (Figure 1). The oil and gas survey in this area suggested that the Jinyang Basin is a petroliferous basin with significant resource potentials, and the most significant hydrocarbon source rock is the early Jurassic Beipiao Formation. Of the four geological survey wells (SZK01-04) drilled on the western margin of Jinyang basin, oil and gas were encountered in three of them [34]. The YD-1 well drilled in the Zhangjiyingzi depression of the basin encountered oil spots in the fractures of volcanic rocks. Based on biomarker and source rock correlation studies, the crude oil was found from the early Jurassic Beipiao Formation, especially Beipiao source rocks in the Wolong section [35].

Most of the outcrops of the Beipiao Formation experienced igneous intrusions in forms such as dykes, sills, and plugs. The anomalous heat, to some extent like "baking effect," is significant. However, the extent of the altered width (thermal aureoles) induced by the igneous activity, and its impact on hydrocarbon generation and expulsion in the basin are not well known in this area. In this study, we documented organic-geochemical changes in systematically collected samples within the thermal aureole close to the intrusive body. The changes recorded in organic geochemical parameters such as R_0, T_{max}, PI, and HI were presented in relation to the distance from dyke intrusion. This work intends to make clear the factors that determine the width of contact aureole and understand the factors that affect hydrocarbon expulsion efficiency in the vicinity of igneous intrusions.

2 Geological settings

2.1 Geological settings of Jinyang Basin and Beipiao Formation

The Jinyang basin is one of the four NE elongated early Mesozoic terrestrial basins in western Liaoning province, China. The Jinyang basin is bounded by the Nantianmen thrust fault to the west and border on the Beipiao basin and Chaoyang-Jianchang basin from north to south [36]. The Jinyang basin is about 200 km long and 40 km wide and covers an area about 7,400 km^2. The basin-fills mainly include a suite of Mesozoic terrestrial clastic deposits, volcanics, and pyroclastic rocks. It is the basin with the most developed Jurassic deposits in north China. Over 90% of the Jinyang basin is covered with middle and upper Jurassic volcano sedimentary successions, forming the most of the sedimentary sequences in this basin [37]. The Mesozoic basin-fill sequences in Jinyang basin start with lava and pyroclastic rocks and end with thick coarse clastic rocks and/or conglomerates, showing cyclic basin development controlled by geotectonic mechanism [38].

The Jinyang basin was formed as a result of the large-scale lithospheric thinning under extensional tectonic settings during early Mesozoic and then undergone compressional settings in late Jurassic time [39–42]. Located on the eastern North China Craton, it remained relatively quiescent from the late Paleoproterozoic until Mesozoic times. Voluminous Jurassic–Cretaceous volcanic rocks erupted and hence formed a series of small Mesozoic basins including the Jinyang basin (Figure 1). Early to late Jurassic mafic to intermediate volcanism was widespread across the Yanshan area, but reached its maximum intensity in the Late Jurassic and Early Cretaceous [43].

The early Jurassic Beipiao Formation, the focus of this study, was considered to be the most significant organic rich source rock in the Jinyang basin. Although there was extensive volcanism during Jurassic times, the Beipiao Formation was deposited during periods without much volcanism. The Beipiao Formation is a coal-bearing unit and consists of alternating fluvial lacustrine shale, sandy shale with sandstone, conglomerate, and coal-bearing layers. However, only few outcrops of Beipiao Formation can be found in the Jinyang basin, and most of the outcrops occur on the western area near the Nantianmen thrust fault, including Kuntouyingzi area, Wolong area, and the Sanbao coal pit. The oil and

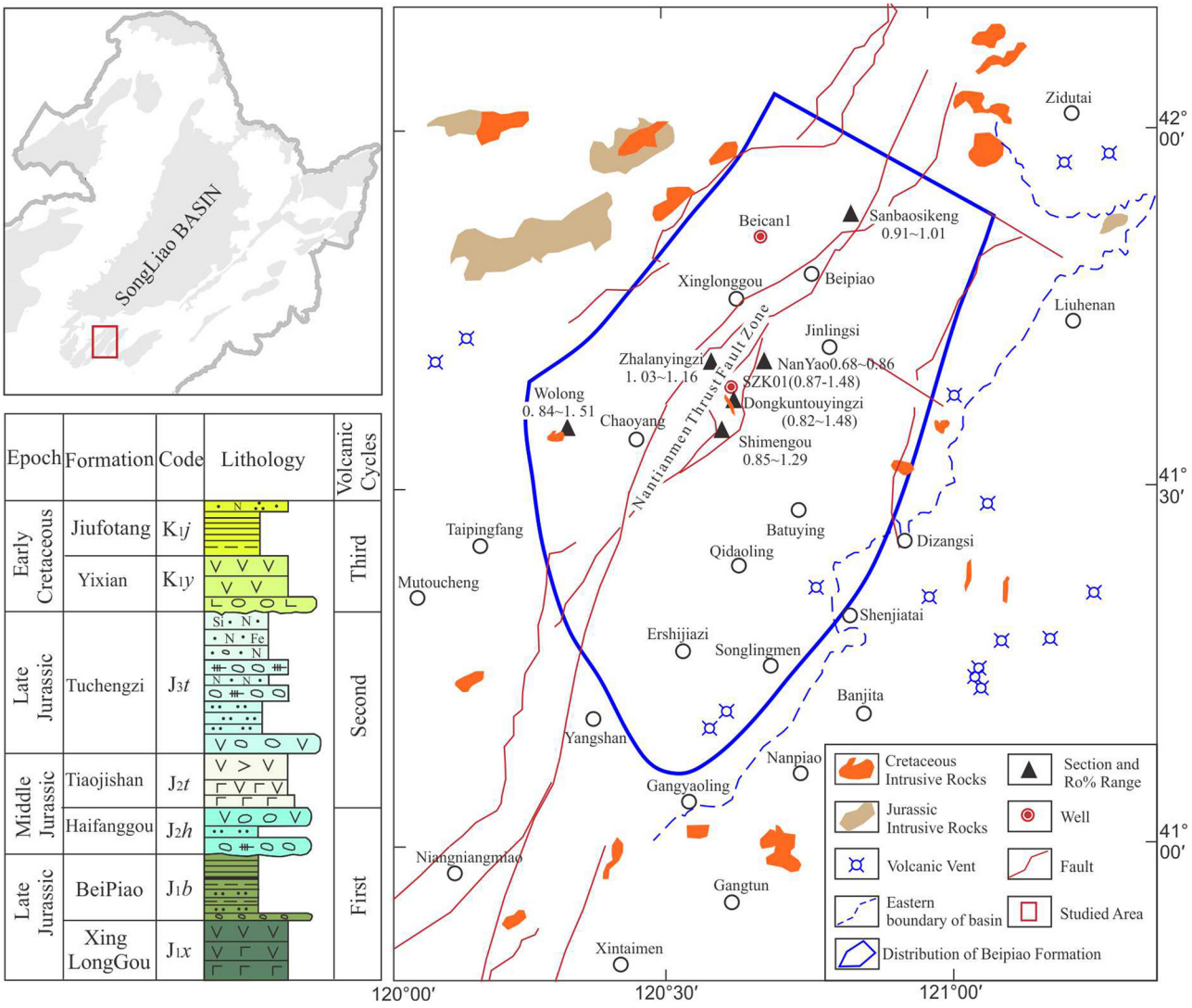

Figure 1: Location of the study area and the distribution of Jurassic and Cretaceous igneous intrusions.

gas exploration in the Jinyang basin conformed that the Beipiao Formation has the potential to generate both oil and gas [35,44–47]. With three volcanic eruption-sedimentary cycles (Figure 1), the magmatic activity in the Jinyang Basin was relatively strong, and the effect of intrusive bodies on the thermal evolution of Beipiao source rock is significant. Igneous intrusions are common in Beipiao Formation, for example, the Wolong section and the Kuntouyingzi section.

The Wolong geological cross section is located in a synclinorium, which was formed during the early Indosinian-Yanshan orogeny stage as indicated in previous studies [37]. The synclinorium has an EW-trending axial trace with a length of 10 km (Figure 2). The west end and the north limbs were cut by faults, and the east side was unconformably overlained by early Crataceous Yixian Formation. The core of the synclinorium is composed of Beipiao Formation with several light gray to brown diorite porphyrite intrusive dykes. The limbs of the synclinorium are composed of the early Jurassic Xinglonggou Formation. The Dongkuntouyingzi geological section is located in Xiaogangou village, about 13 km east of Chaoyang City, with a length of 1.23 km. The main lithology of the Beipiao Formation in the section is green-gray thin-layered fine-grained sandstone interlayered by siltstone, yellow silty mudstone, and dark gray black mudstone. The sections provide a natural laboratory to study the interactive mechanism of the igneous intrusion body and the Beipiao source rock, which can provide insight into the thermal evolution history of the Beipiao source rock.

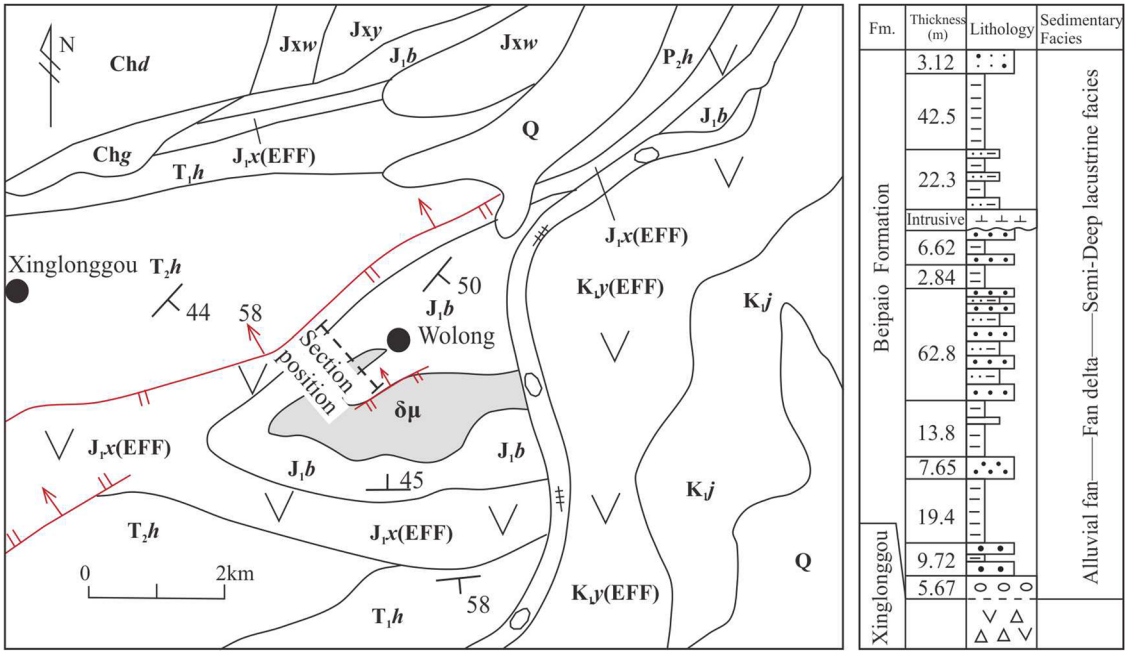

Figure 2: Location of the Wolong section and its stratigraphic column.

2.2 Relationship between host rock and igneous intrusions

Based on the geological cross section measurement, the strata along the Wolong cross section can be subdivided into 12 layers (Figure 2). The detail field observation of the lithological associations and sedimentary structures indicate sedimentary environments of alluvial fan, fan delta, and lacustrine deposits. There are four main black shale layers with a total thickness of about 98 m. The cumulative thickness of the Beipiao group calculated from the Wolong section is about 200 m. Black shale layers in this cross section mostly vary from 10 to 30 m (Figure 3a). The light gray-brown diorite porphyrite is located at the bottom of the ninth layer (Figure 3b) with an exposed thickness about 204 m, which exhibits parallel relationship with the bedding plane. The intrusive body shows a yellow-grey color in the outcrop and has typical spherical weathering characteristics (Figure 3c).

3 Sampling and analytical methods

Eight and eleven organic rich source rock samples of Beipiao Formation were collected from the Wolong and Dongkuntouyingzi cross sections, respectively. Outcrop samples in the Wolong area were collected at the contact of dykes. Shale samples were collected at intervals from 30 to 50 m successively moving away from the intrusive dyke. Fresh samples were collected after excavating about 10 cm of the exposed shale to eliminate the influence of weathering. The samples included only organic rich source rocks, which overlie the intrusive body. The intrusive dyke sample was also collected from the Wolong cross section for the identification of its composition and age (sample ID: pm1602, location: 120°18′22.81″, 41°34′55.77″).

The weathered surfaces of the samples were removed and cleaned before organic geochemical analyses to minimize the effects of weathering and potential contamination. The samples were pulverized to powder for both the Rock-Eval and vitrinite reflectance (R_O) analyses. The TOC analysis was carried out by a LECO CS-200 carbon and sulfur analyzer by following a standardized procedure. Rock–Eval pyrolysis was performed with a Rock–Eval 6 instrument. The temperature program started with an isothermal phase for 3 min at 300°C, followed by a heating step up to 650°C at a rate of 25°C. The analysis and testing of the samples were done in the Key Laboratory of Oil and Gas Resources and Exploration of the Ministry of Education of Yangtze University. The test methods and experimental instruments were based on the Chinese national standard GB/T 18602-2012.

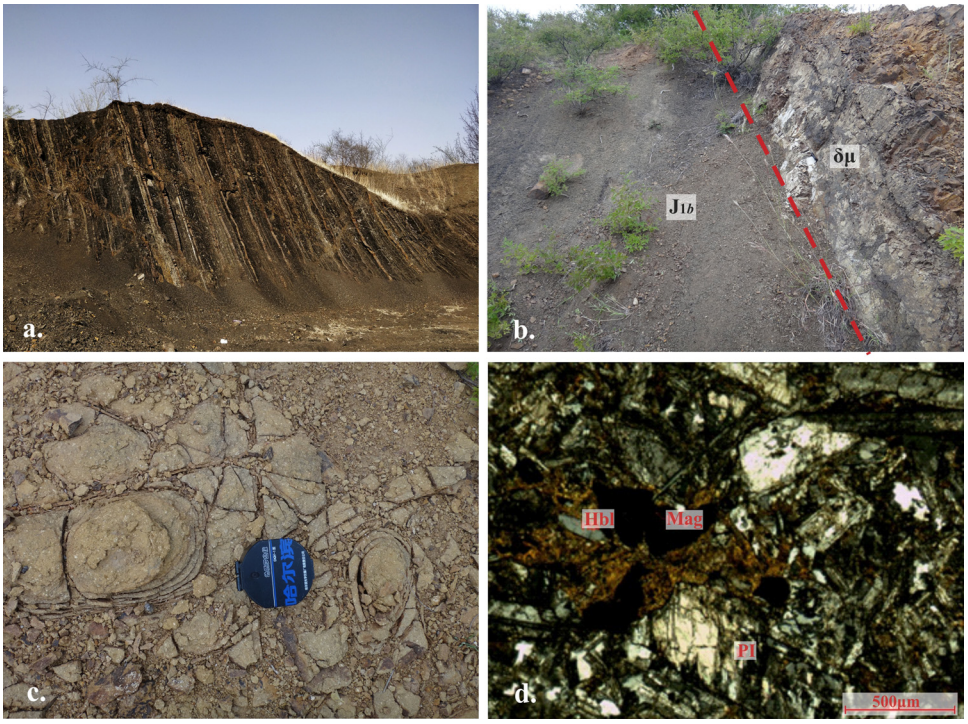

Figure 3: Representative field structures and thin section photomicrograph of diorite porphyry intrusion in the Wolong section. (a) black shales in the outcrop; (b) the contact zone of black shale and diorite porphyry intrusion; (c) the diorite porphyry intrusion show the spheroidal weathering appearance in the outcrop; (d) thin section photomicrograph of diorite porphyry intrusion.

4 Results

4.1 Petrology of igneous intrusions

The intrusive dyke show the spheroidal weathering appearance with yellow to green yellow colors in the field. The petrological results indicate that the dyke is composed of altered quartz diorite porphyrite (Figure 3d). The phanerocrysts are mainly plagioclase and altered hornblende, which vary from 0.4 to 2.5 mm. The plagioclase is mostly subhedral to euhedral grains with platy or columnar form, and the surface is commonly altered with kaolinization, sericitization, and carbonatization. The hornblende grains are mostly metasomatized by carbonate minerals and biotite aggregates, retaining hornblende crystal form, present as pseudomorphs. The matrix is mainly composed of plagioclase, altered hornblende, biotite, and quartz. The mineral grains are less than 0.25 mm. The space between the disordered plagioclase grains are filled with other altered minerals. All these features suggest a hypabyssal intrusive face, which is also in accordance with the deduction that the igneous intrusions were emplaced during the early stage of diagenesis of the Beipiao Formation.

4.2 Changes in shale micro-texture

Based on the degree of metamorphism, we divide the samples into three groups, unaltered, mildly altered, and extremely altered. The unaltered samples are characterized by planar and wrinkled laminae in their microstructures (Figure 4a and b). The organic matters in the unaltered shales exhibit thin, continuous to discontinuous streaks. The mildly altered shale samples have darker organic matter compared with samples from the unaltered area (Figure 4c and d). Most of the organic matters in this area keep their original micro fabric structures. The samples of the extremely altered area nearly lost all the micro fabric details. The organic matters in this area have much small size and occur sporadically in the matrix of the silts (Figure 4e and f).

4.3 Organic geochemistry of Beipiao shale

Various organic geochemical parameters tests were carried out for 154 drilling core samples, 164 shale samples from three measured geological sections, and 37 samples from four geological sections collected for comparisons and data analysis [48]. The organic rich

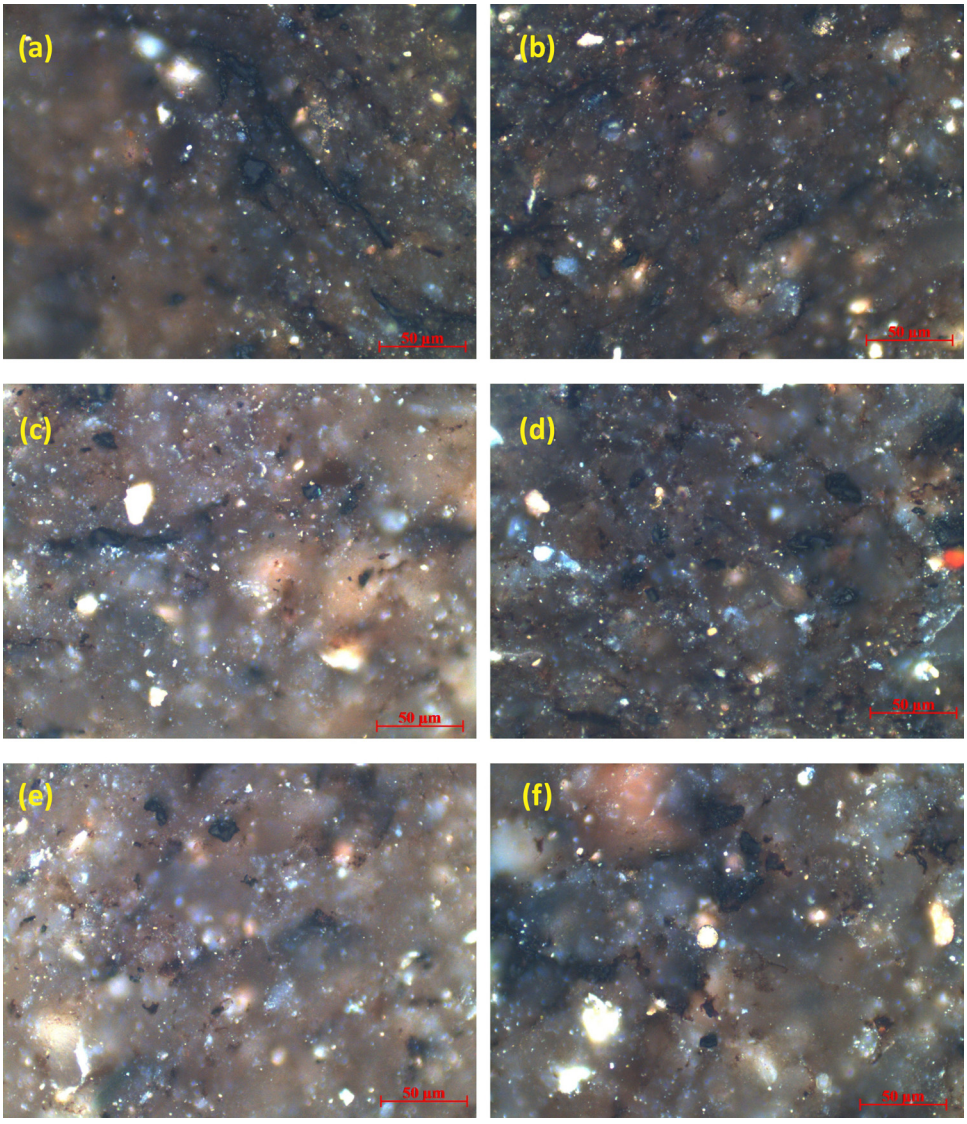

Figure 4: (a–f) Micrographs of samples in different zones, extremely altered samples (a and b), mildly altered samples (c and d), and unaltered samples (e and f).

source rocks from the Beipiao Formation, which were not affected by intrusive bodies in the Jinyang Basin were also analyzed (Table 1). The results show that the TOC value varies from 0.03% to 14.1% with an average of 1.19%. The pyrolysis hydrocarbon generational potential ($S_1 + S_2$) distributes in a range of 0.01–14.82 mg/g with an average of 1.61 mg/g. The T_{max} value ranges from 322°C to 563°C, with an average of 469.74°C. The R_0 value ranges from 0.6% to 1.54%, with an average of 0.94%. These parameters suggest that the Beipiao source rocks are in the mature stage and are basically fair to good source rocks, except for few samples, which are poor source rocks. However, it should be noted that high maturity and weathering may be cause of the extremely low potential for some samples, especially for samples in the exact vicinity of the intrusive body (Table 2). It can be concluded that the primary hydrocarbon potential is better than the analyzed results.

5 Discussions

5.1 Width of altered zone

It is of great significance to understand the extent of thermal influence of intrusions on surrounding rocks. Numerous studies had illustrated that the thickness of contact metamorphism aureoles depends on factors such

Table 1: Organic geochemical data of Beipiao source rock from Jinyang Basin

Locations (well no.)	Lithology	TOC/%	T_{max}/°C	$S_1 + S_2$/mg g^{-1}	R_0/%
Average		1.91(201)	469.74(186)	1.61(201)	0.94(57)
Dongkuntouyingzi*	Black mudstone	0.521–4.75	441–458	0.02–3.13	0.6–1.15
		1.69(13)	450(5)	0.69(13)	0.78(10)
Shimengou*	Black mudstone	0.03–4.55	447–546	0.13–2.13	0.85–1.29
		2.11(17)	495(17)	0.78(17)	1.05(17)
Nanpiao Yanjialing*	Black mudstone	0.96–1.22	526–532	0.01–0.03	—
		1.07(3)	529(3)	0.017(3)	
Batuying Diaojiagou*	Black mudstone	0.12–0.20		0.01–0.03	—
		0.37(4)		0.018(4)	
Nanbajia Nanyao	Black mudstone	1.32–4.83		0.01–0.36	0.68–0.86
		2.50(3)		0.17(3)	0.75(3)
Beipiao Sanbaosikeng	Light-black mudstone	0.06–0.295	437–452	0.02–0.13	0.91–1.01
		0.18(2)	445(2)	0.08(2)	0.96(2)
Taohuatu Zhalanyingzi	Black mudstone	1.28–7.51	414–558	0.04–1.55	1.03–1.16
		2.59(5)	475(5)	0.57(5)	1.09(5)
SZK01	Black mudstone	0.16–4.35	385–546	0.03–7.29	0.78–1.54
		1.32(44)	463(44)	1.35(44)	0.90(17)
SZK02	Black carbonaceous mudstone	1.21–4.53	322–503	0.05–14.82	0.87–1.18
		2.72(51)	453(51)	2.78(51)	1.05(3)
SZK03	Black mudstone	0.34–14.1	448–563	0.23–8.66	—
		1.77(59)	481(59)	1.65(59)	

*Asterisks denote the data were collected from literature [36].

Table 2: Organic geochemical data of Beipiao source rock from Wolong and Kuntouyingzi profile

No.	Sample	Lithology	Distance/m	TOC/%	T_{max}/°C	$S_1 + S_2$/mg g^{-1}	PI	R_0/%
1	WL-1	Black shale	29	2.18	573	0.28	0.32	1.45
2	WL-2	Black shale	46	3.2	558	0.17	0.29	1.51
3	WL-3	Black shale	94	2.9	531	0.11	0.27	1.43
4	WL-4	Black shale	114	2.57	447	0.21	0.29	0.97
5	WL-5	Black shale	150	1.29	471	0.3	0.37	1.13
6	WL-6	Black shale	250	1.63	427	0.07	0.43	0.84
7	WL-7	Black shale	300	1.68	430	0.14	0.29	0.86
8	WL-8	Black shale	335	0.605	472	0.05	0.40	1.14
9	GG-1	Black shale	325	0.57	444	0.74	0.18	1.11
10	GG-2	Black shale	340	0.70	444	0.34	0.18	1.14
11	GG-3	Black shale	360	0.67	447	1.33	0.19	1.14
12	GG-4	Black shale	370	1.13	450	1.36	0.15	1.09
13	GG-5	Black shale	390	0.76	470	0.23	0.17	1.08
14	GG-6	Black shale	450	1.11	446	1.38	0.12	1.02
15	GG-7	Black shale	460	0.89	444	0.47	0.26	0.97
16	GG-8	Black shale	570	0.72	447	1.06	0.08	0.86
17	GG-9	Black shale	620	1.34	448	2.99	0.10	0.86
18	GG-10	Black shale	740	1.35	446	1.37	0.10	0.82

as thickness, size, temperature of magma, thermal properties of the host rock, thermal effects of water or metamorphism in the host rock, as well as the style of heat transfer [1,3,4,24,31,49,50]. The heat source from igneous intrusions had strong influence on the transformation of organic matter in the organic rich host rock and can also promote hydrocarbon generation process. In some cases, such as igneous intrusions emplaced into immature source rock, the igneous activity can generate the heat required to mature otherwise immature. Based on the different conditions and assumptions, previous studies indicate that the extent of thermal aureole is

varied. In most cases studied, the thermal effect of igneous bodies intruded into sedimentary rocks is expected to be one to two times the thickness of the intrusion body [31,51–54]. Based on the published literatures and numerical modeling results, Aarnes et al. summarized that aureole thicknesses can vary from 30% to 250% of the sill thickness depending on host-rock temperature, sill thickness, and intrusion temperature [1]. Recently, Bulguroglu and Milkov reported that the relatively thin (<5 m) sills have aureole thicknesses of 276 to >1,000% of the sill thickness, significantly larger than the previously reported from most other locations affected by igneous intrusions [55]. However, these results were later questioned by other numerical modeling results, suggested that the aureole was exaggerated by low-resolution mesh, and concluded that an aureole thickness of 30%–200% of the sill thickness is applicable [54].

According to the variations of R_0 values of the samples analyzed, R_0 value of 0.95% is common across various sections and wells. Therefore, R_0 value of 0.95% is used as the background value to study the thermal aureole of the intrusive body for Wolong section. Similarly, the T_{max} value of 470°C is also used in this study to determine the extent of influence of the anomalous heat. The extremely altered zone is characterized by the complete loss of micro-texture because of charcoalization of the organic matter (Figure 4). Micro-textural details of the samples from the background area remain unaltered and keep almost all micro-textures, while samples from mildly altered zone record minor modifications of the texture. As indicated by the cross plot of T_{max}/R_0 and distance from the intrusive body (Figure 5), both the R_0 and T_{max} values reduce sharply in a few meters near to the intrusive body. As the distance from the contact zone reaches to about 200 m, both the R_0 and T_{max} values are stabilized and decrease to the regional background values (Figure 5). The cause of relatively high R_0 value in the range of 300–500 m is not well defined. Hence, the high R_0 values might include but not limited to weathering, heterogeneity of shales, and personal factors when measuring the vitrinite reflectance.

This width of the altered zone is consistent with the facts reported by other literature. As mentioned earlier, the extent of influence of the intrusive body is closely related to the scale of the intrusive body. In this study, the relatively thin aureole indicates that the heat brought by the magma is conducted mainly by a pure conductive model. Hydrothermal convection is limited in the host rock during the time of the igneous body intrusion and maybe related to the diagenetic stage of the surrounding source rocks. When the body in the Wolong section was formed (U–Pb age: 164.4 ± 1.5 Ma), the source rocks of the Beipiao Formation were still in the early diagenetic stage. The thermal conductivity is relatively low and specific heat capacity of the sedimentary deposits is high. The source rock in the vicinity of the intrusive body absorbed the majority of heat from the intrusive body, which led to the relatively narrow extent of influence of magma intrusion on the maturity of the source rock. In summary, the extent of influence of the anomalous heat of the intrusive rock on the surrounding rock is not only affected by the initial temperature and scale of the intrusive body but also related to the diagenetic stage of the surrounding rock.

5.2 Effects of igneous intrusions on hydrocarbon generation

With the increasing thermal maturity, the TOC values of source rocks will be progressively diminished due to generation and discharge of hydrocarbon from source rocks. When comparing samples from the two sections, it is observed that all samples have relatively high TOC value, the closer the samples to the intrusive body, the lower the hydrocarbon generation potential ($S_1 + S_2$) and hydrogen index (HI) (Figure 6). In addition, for samples in the exact vicinity of the intrusive body, the chloroform asphalt "A" content and total hydrocarbon content are lower than 0.015% and 100 μg/g, respectively, indicating nonhydrocarbon source rock. These results suggest that the anomalous heat from the intrusive body can not only promote the maturity process of source rocks but also can reduce the abundance of the residual organic matter in the source rocks and can even make nonhydrocarbon source rocks.

Judging by the PI-T_{max} diagram (Figure 7), most of the samples have entered the oil window, and large-scale hydrocarbon expulsion had took place. There is not an obvious trend for the T_{max} value and PI value, where a clearly positive relationship is often seen in other areas. Our explanation for this phenomenon is migration of hydrocarbon in the shales. For samples nearer (<100 m) to the intrusive body, almost all the generation potentials had been exhausted and all have very low S_2 values. However, there may be still some amount of free hydrocarbon (S_1) present and hence may yield relatively high PI in the nearby area. For samples in the oil window, a clear negative relationship between the PI

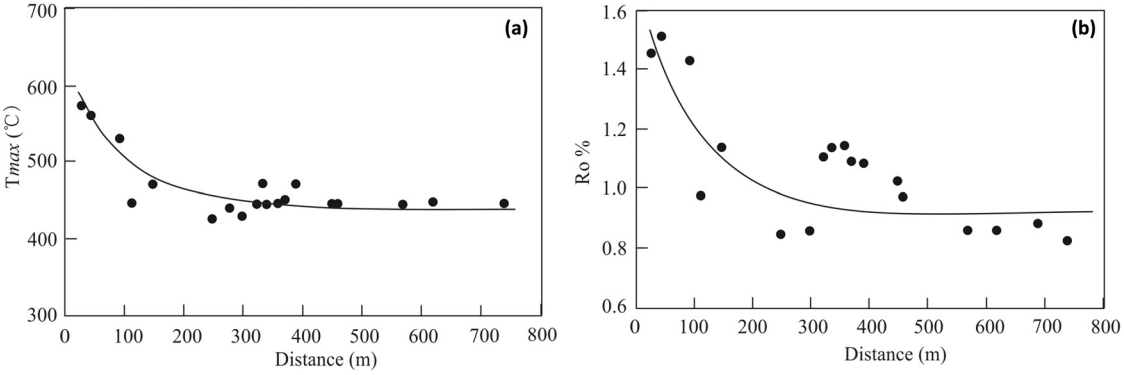

Figure 5: T_{max} values (a) and R_o values (b) as a function of distance from the dyke margin.

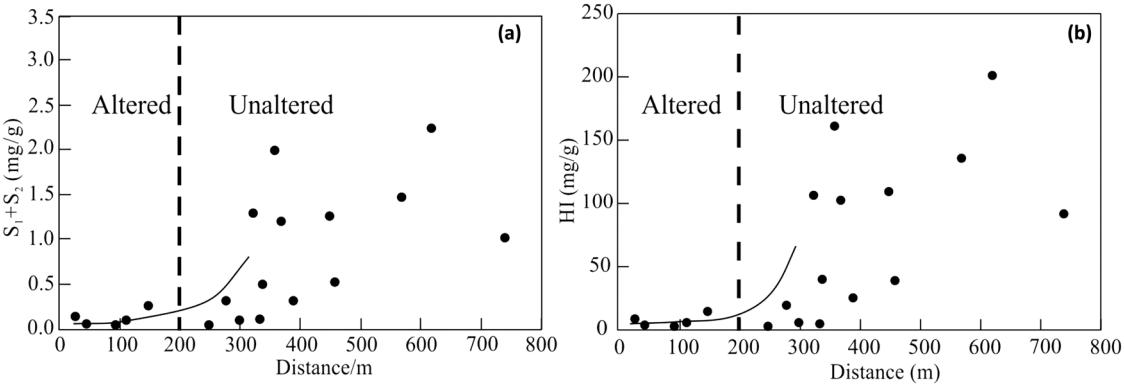

Figure 6: Cross plot of $S_1 + S_2$ (a) and HI (b) versus distance from the intrusion body.

and distance to the contact zone is seen (Figure 7), i.e., samples in this area have abnormally high free hydrocarbon. It can be concluded that these hydrocarbons were migrated from the high maturity area near the contact zone due to the fluid overpressure [57]. The heating effect is negligible at distance faraway from the intrusive body, where due to relatively low maturity level, only limited free hydrocarbons were generated and hence have the lowest PI values. If this deduction is true, then it can be inferred that the igneous intrusion in this area has beneficial effect on the accumulation and storage properties of the shales. In fact, these phenomena are not rare and have been reported in many other areas. Saghafi et al. reported that in South African coal seams, the effect of the igneous intrusions had enhanced the gas release and storage of these coals [58]. In the Illinois Basin, in the altered zone, strong reduction in mesopore and micropore volumes was observed, which has a negative effect on the adsorption of gas [18]. However, in the Daxing Mine, China, increased porosity, pore volume, and average pore diameter were found in the thermally altered area due to igneous intrusions, and the transport capacity is increased [59]. Based on study of changes of coal organic composition and pores/fractures resulting from igneous intrusions, Yao and Liu pointed out that influence of igneous intrusion on coal pores and fractures vary significantly depending on the intrusion type, the rank after the intrusion, and the nature of the sediments being intruded [22]. Correspondingly, as a main topic of shale gas evaluation, it has been reported that due to the generation and expulsion of hydrocarbons from organic matters, the pore volumes generally show a positive relationship with thermal maturity [60–65]. Combined with the fact that hydrocarbon generation conversion rates are inversely proportional to the distance from the intrusion for samples in the oil-producing window, we can prudently draw the deduction that the additional free hydrocarbon has migrated from the high maturity areas.

For the samples in the oil-producing window, their hydrocarbon generation conversion rates are inversely proportional to the distance from the intrusion to the samples (Figure 7). Three samples about 500–800 m from the intrusive body have a very low conversion

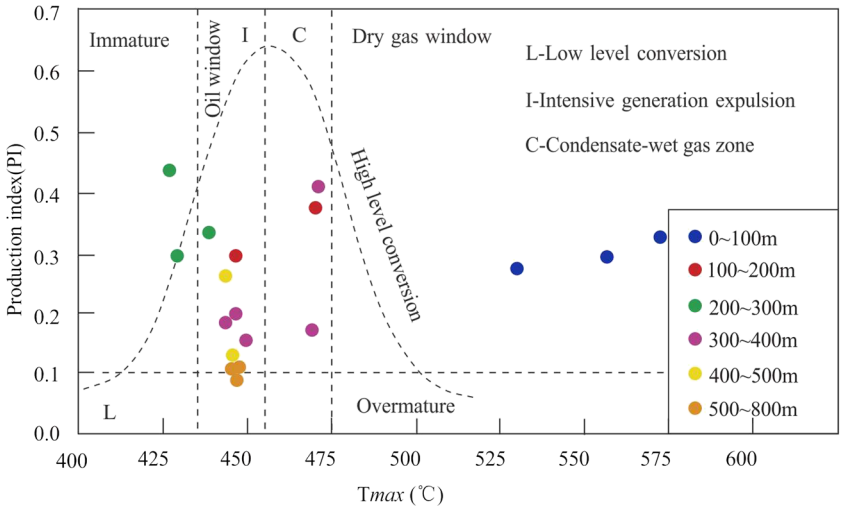

Figure 7: Plot of PI versus T_{max} values of Beipiao source rock from Wolong and Kuntouyingzi sections. Modified from Waples [56].

stage. The results show that due to the influence of the anomalous heat from the intrusive body, the hydrocarbon conversion rate of the source rocks is greatly increased. In this case, the igneous intrusions in the Jinyang Basin might have promoted the generation and expulsion of hydrocarbons from the source rocks and greatly improved the production index. These results can provide useful evidences for the understanding of oil and gas formation processes in the Jinyang Basin. This observation can also provide useful basis for the prediction of resource potential and promising exploration blocks in the Jinyang basin.

6 Conclusions

In this study, a comprehensive investigation of the organic geochemistry of the shale of the Beipiao Formation intruded by the diorite intrusive body was conducted. The main conclusions are listed as follows:

Thermal effect of the Mesozoic intrusive body in the Jinyang Basin caused maturation of source rock of the Beipiao Formation. R_O and Rock-Eval T_{max} profiles indicate increasing thermal maturation toward the intrusive body from about one time of the thickness of intrusive body. No thermal convection effect is observed in the contact thermal aureole. The main factors influence the width of altered zone including the initial temperature and scale of the intrusive body and the diagenetic stage of surrounding rock in the Jinyang Basin. Organic geochemical results support increasing hydrocarbon generation intensity from the organic matter toward the intrusive body. The production index reached its peak value at about one time of the intrusive body thickness, approximately same as the thickness of the aureole area. Free hydrocarbon migration from high maturity areas to relatively low maturity areas could have been occurred due to the fluid overpressure. The loss of organic carbon has resulted in the formation of better accumulation properties and storage capacities of the shales in the Beipiao Formation.

Acknowledgments: This study was financially supported by National Natural Science of China (Grant No. 41790451) and China Geological Survey oil and gas survey program (Grant No. DD20190098). We appreciate the constructive and thoughtful comments by two anonymous reviewers that greatly improved the paper.

Author contributions: Tao Zhang conceived of the presented idea and planned the experiments. Shouliang Sun and Tao Zhang wrote the manuscript. Shouliang Sun contributed to the interpretation of the results and directed the project. Yongfei Li and Shuwang Chen were involved in planning and supervised the work. Qiushi Sun performed the experiments and calculations of some of the indexes. All authors discussed the results and commented on the manuscript.

References

[1] Aarnes I, Svensen H, Connolly JAD, Podladchikov YY. How contact metamorphism can trigger global climate changes:

modeling gas generation around igneous sills in sedimentary basins. Geochim Cosmochim Acta. 2010;74:7179–95. doi: 10.1016/j.gca.2010.09.011.

[2] Alalade B, Tyson RV. Influence of igneous intrusions on thermal maturity of Late Cretaceous shales in the Tuma well, Chad Basin, NE Nigeria. J Afr Earth Sci. 2013;77:59–66. doi: 10.1016/j.jafrearsci.2012.09.006.

[3] Barker CE, Bone Y, Lewan MD. Fluid inclusion and vitrinite-reflectance geothermometry compared to heat-flow models of maximum paleotemperature next to dikes, western onshore Gippsland Basin, Australia. India. Int J Coal Geol. 1998;37:73–111. doi: 10.1016/S0166-5162(98)00018-4.

[4] Galushkin YI. Thermal effects of igneous intrusions on maturity of organic matter, A possible mechanism of intrusion. Org Geochem. 1997;26:645–58. doi: 10.1016/S0146-6380(97)00030-2.

[5] Jaeger JC. Thermal effects of intrusions. Rev Geophys. 1964;2:443. doi: 10.1029/RG002i003p00443.

[6] Liu E, Wang H, Tonguç Uysal I, Zhao J, Wang X, Feng Y, et al. Paleogene igneous intrusion and its effect on thermal maturity of organic-rich mudstones in the Beibuwan Basin, South China Sea. Mar Pet Geol. 2017;86:733–50. doi: 10.1016/j.marpetgeo.2017.06.026.

[7] Othman R, Arouri KR, Ward CR, McKirdy DM. Oil generation by igneous intrusions in the northern Gunnedah Basin, Australia. Org Geochem. 2001;32:1219–32. doi: 10.1016/S0146-6380(01)00089-4.

[8] Santos RV, Dantas EL, Oliveira CGD, Alvarenga CJSD, Anjos CWDD, Guimarães EM. Geochemical and thermal effects of a basic sill on black shales and limestones of the Permian Irati Formation. J South Am Earth Sci. 2009;28:14–24. doi: 10.1016/j.jsames.2008.12.002.

[9] Spacapan JB, Palma JO, Galland O, Manceda R, Rocha E, D'Odorico A. Thermal impact of igneous sill-complexes on organic-rich formations and implications for petroleum systems, A case study in the northern Neuquén Basin, Argentina. Mar Pet Geol. 2018;91:519–31. doi: 10.1016/j.marpetgeo.2018.01.018.

[10] Sun Y, Fu J, Liu D, Sheng G, Chen Z, Wu T. Effect of volcanism on maturation of sedimentary organic matter and its significance for hydrocarbon generation, a case:the East Sag of Liaohe Basin. Chin Sci Bull. 1995;17:1446–50 (in Chinese with English abstract).

[11] Sydnes M, Fjeldskaar W, Løtveit IF, Grunnaleite I, Cardozo N. The importance of sill thickness and timing of sill emplacement on hydrocarbon maturation. Mar Pet Geol. 2018;89:500–14. doi: 10.1016/j.marpetgeo.2017.10.017.

[12] Aarnes I, Fristad K, Planke S, Svensen H. The impact of host-rock composition on devolatilization of sedimentary rocks during contact metamorphism around mafic sheet intrusions. Geochem Geophys Geosyst. 2011;12:1–11. doi: 10.1029/2011GC003636.

[13] Arora A, Dutta S, Gogoi B, Banerjee S. The effects of igneous dike intrusion on organic geochemistry of black shale and its implications, Late Jurassic Jhuran Formation, India. Int J Coal Geol. 2017;178:84–99. doi: 10.1016/j.coal.2017.05.002.

[14] Chen J, Liu G, Li H, Wu B. Mineralogical and geochemical responses of coal to igneous intrusion in the Pansan Coal Mine of the Huainan coalfield, Anhui, China. Int J Coal Geol. 2014;124:11–35. doi: 10.1016/j.coal.2013.12.018.

[15] Dun W, Guijian L, Ruoyu S, Shancheng C. Influences of magmatic intrusion on the macromolecular and pore structures of coal: evidences from Raman spectroscopy and atomic force microscopy. Fuel. 2014;119:191–201. doi: 10.1016/j.fuel.2013.11.012.

[16] Farrimond P, Bevan JC, Bishop AN. Hopanoid hydrocarbon maturation by an igneous intrusion. Org Geochem. 1996;25:149–64. doi: 10.1016/S0146-6380(96)00128-3.

[17] Jiang J, Cheng Y, Wang L, Li W, Wang L. Petrographic and geochemical effects of sill intrusions on coal and their implications for gas outbursts in the Wolonghu Mine, Huaibei Coalfield, China. Int J Coal Geol. 2011;88:55–66. doi: 10.1016/j.coal.2011.08.007.

[18] Mastalerz M, Drobniak A, Schimmelmann A. Changes in optical properties, chemistry, and micropore and mesopore characteristics of bituminous coal at the contact with dikes in the Illinois Basin. Int J Coal Geol. 2009;77:310–9. doi: 10.1016/j.coal.2008.05.014.

[19] Presswood SM, Rimmer SM, Anderson KB, Filiberto J. Geochemical and petrographic alteration of rapidly heated coals from the Herrin (No. 6) Coal Seam, Illinois Basin. Int J Coal Geol. 2016;165:243–56. doi: 10.1016/j.coal.2016.08.022.

[20] Sarana S, Kar R. Effect of igneous intrusive on coal microconstituents: Study from an Indian Gondwana coalfield. Int J Coal Geol. 2011;85:161–7. doi: 10.1016/j.coal.2010.11.006.

[21] Yang M, Liu G, Sun R, Chou C, Zheng L. Characterization of intrusive rocks and REE geochemistry of coals from the Zhuji Coal Mine, Huainan Coalfield, Anhui, China. Int J Coal Geol. 2012;94:283–95. doi: 10.1016/j.coal.2011.06.012.

[22] Yao Y, Liu D. Effects of igneous intrusions on coal petrology, pore-fracture and coalbed methane characteristics in Hongyang, Handan and Huaibei coalfields, North China. Int J Coal Geol. 2012;96–97:72–81. doi: 10.1016/j.coal.2012.03.007.

[23] Iyer K, Schmid DW, Planke S, Millett J. Modelling hydrothermal venting in volcanic sedimentary basins: impact on hydrocarbon maturation and paleoclimate. Earth Planet Sci Lett. 2017;467:30–42. doi: 10.1016/j.epsl.2017.03.023.

[24] Iyer K, Svensen H, Schmid DW. SILLi 1.0: a 1-D numerical tool quantifying the thermal effects of sill intrusions. Geosci Model Dev. 2018;11:43–60. doi: 10.5194/gmd-11-43-2018.

[25] Wang D, Song Y, Xu H, Ma X, Zhao M. Numerical modeling of thermal evolution in the contact aureole of a 0.9 m thick dolerite dike in the Jurassic siltstone section from Isle of Skye, Scotland. J Appl Geophys. 2013;89:134–40. doi: 10.1016/j.jappgeo.2012.12.004.

[26] Aarnes I, Planke S, Trulsvik M, Svensen H. Contact metamorphism and thermogenic gas generation in the Vøring and Møre basins, offshore Norway, during the Paleocene–Eocene thermal maximum. J Geol Soc. 2015;172:588–98. doi: 10.1144/jgs2014-098.

[27] Svensen HH, Iyer K, Schmid DW, Mazzini A. Modelling of gas generation following emplacement of an igneous sill below Lusi, East Java, Indonesia. Mar Pet Geol. 2018;90:201–8. doi: 10.1016/j.marpetgeo.2017.07.007.

[28] Svensen H, Planke S, Malthe-Sørenssen A, Jamtveit B, Myklebust R, Rasmussen Eidem T. Release of methane from a volcanic basin as a mechanism for initial Eocene global

warming. Nature. 2004;429:542–5. doi: 10.1038/nature02566.
[29] Adeniyi EO, Ossa Ossa F, Kramers JD, de Kock MO, Belyanin G, Beukes NJ. Cause and timing of the thermal over-maturation of hydrocarbon source rocks of the Ecca Group (Main Karoo Basin, South Africa). Mar Pet Geol. 2018;91:480–500. doi: 10.1016/j.marpetgeo.2018.01.033.
[30] Costin G, Götz AE, Ruckwied K. Sedimentary organic matter characterization of the Whitehill shales (Karoo Basin, South Africa): An integrated quantitative approach using FE-EPMA and LA-ICP-MS. Rev Palaeobot Palynol. 2019;268:29–42. doi: 10.1016/j.revpalbo.2019.05.008.
[31] Dow WG. Kerogen studies and geological interpretations. J Geochem Explor. 1977;7:79–99. doi: 10.1016/0375-6742(77)90078-4.
[32] Iyer K, Rüpke L, Galerne CY. Modeling fluid flow in sedimentary basins with sill intrusions: Implications for hydrothermal venting and climate change. Geochem Geophys Geosyst. 2013;14:5244–62. doi: 10.1002/2013GC005012.
[33] Zhang X. Mechenism of basin and evaluation of oil gas in Mesozoic down faulted basin in northeast China: thesis. Jilin University; 2007 (in Chinese with English abstract).
[34] Li Y, Chen S. A new discovery of oil and gas in Jinyang Basin, western Liaoning province. Geol Bull China. 2014;33:1463–4 (in Chinese with English abstract).
[35] Zhang T, Li Y, Sun S, Gao X, Zhou T, Sun P. Saturated hydrocarbon geochemical characteristics of the oil sand from YD1 well in Jinyang Basin and its significance for oil and gas exploration. Geol Bull China. 2017;36:582–90 (in Chinese with English abstract).
[36] He B, Fu Q, Zhang Y. Beipiao group hydrocarbon material distribution and organic matter abundance of Jinlingsi – Yangshan basin in western part of Liaoning. J Liaoning Technical Univ. 2006;25:24–7 (in Chinese with English abstract).
[37] Huang Z, Pan Y, Yang Y, Liu W, Dan X. Regional geological survey report of 1:250,000 zone in Jinzhou, Liaoning. Liaoning Provincial Institute of Geology and Mineral Resources Investigation; 2003 (in Chinese with English abstract).
[38] Li Z, Liu S, Zhang J, Wang Q. Typical basin-fill sequences and basin migration in Yanshan, North China – Response to Mesozoic tectonic transition. Sci China Ser D Earth Sci. 2004;47:181–92. doi: 10.1360/02yd0412.
[39] Meng Q, Wu G, Fan L, Wei H. Tectonic evolution of early Mesozoic sedimentary basins in the North China block. Earth Sci Rev. 2019;190:416–38. doi: 10.1016/j.earscirev.2018.12.003.
[40] Wilde SA, Zhou X, Nemchin AA, Sun M. Mesozoic crust-mantle interaction beneath the North China craton: a consequence of the dispersal of Gondwanaland and accretion of Asia. Geology. 2003;31:817–20. doi: 10.1130/G19489.1.
[41] Zhu R, Yang J, Wu F. Timing of destruction of the North China Craton. Lithos. 2012;149:51–60. doi: 10.1016/j.lithos.2012.05.013.
[42] He Z, Niu B, Zhang X. Late Jurassic thrusting and syntectonic sedimentary basin systems in the Chaoyang region, western Liaoning. Geol Rev. 2007;53:152–63 + 295–6 (in Chinese with English abstract).
[43] Davis GA, Yadong Z, Cong W, Darby BJ, Changhou Z, Gehrels G. Mesozoic tectonic evolution of the Yanshan fold and thrust belt, with emphasis on Hebei and Liaoning provinces, northern China. Geol Soc Am Mem. 2001;194:171–97. doi: 10.1130/0-8137-1194-0.171.
[44] Sun Q, Zhang K, Li Y, Gao X, Sun S, Zhang T, et al. Characteristics and implication of biomarker compounds in source rocks from Beipiao Formation in Jinyang basin, western liaoning province. Geol Resour. 2018;27(01):69–76 (in Chinese with English abstract).
[45] Sun S, Li Y, Chen S, Gao X, Sun Q, Zhang K, et al. Depositional environment and organic geochemical characteristics of source rocks of Beipiao Formation in Jinyang Basin: Global. Geology. 2017;36:889–902 (in Chinese with English abstract).
[46] Sun S, Li Y, Gao X, Zhou T, Zhang T, Wang S. An analysis of the genesis and geochemical characteristics of shale gas in Lower Jurassic Beipiao Formation in Jinyang Basin. Geol Bull China. 2017;36:575–81 (in Chinese with English abstract).
[47] Zhen Z, Li Y, Gao X, Sun S, Zhou T. Characteristics of sedimentary facies and organic matter of Lower Jurassic Beipiao Formation of Well SZK01 in Jinyang Basin. Glob Geol. 2016;35:207–15 (in Chinese with English abstract).
[48] Fan X. The analysis and evaluation of petroleum geological condition in Jinlingsi-Yangshan Basin. Fuxin: Liaoning Technical University; 2004 (in Chinese with English abstract).
[49] Aghaei H, Gurba LW, Ward CR, Hall M, Mahmud SA. Effects of igneous intrusions on thermal maturity of carbonaceous fluvial sediments: a case study of the Early Cretaceous Strzelecki Group in west Gippsland, Victoria, Australia. Int J Coal Geol. 2015;152:68–77. doi: 10.1016/j.coal.2015.10.002.
[50] Wang D. Comparable study on the effect of errors and uncertainties of heat transfer models on quantitative evaluation of thermal alteration in contact metamorphic aureoles: thermophysical parameters, intrusion mechanism, pore-water volatilization and mathematical equations. Int J Coal Geol. 2012;95:12–19. doi: 10.1016/j.coal.2012.02.002.
[51] Agirrezabala LM, Permanyer A, Suárez-Ruiz I, Dorronsoro C. Contact metamorphism of organic-rich mudstones and carbon release around a magmatic sill in the Basque-Cantabrian Basin, western Pyrenees. Org Geochem. 2014;69:26–35. doi: 10.1016/j.orggeochem.2014.01.014.
[52] Bishop AN, Abbott GD. Vitrinite reflectance and molecular geochemistry of Jurassic sediments: the influence of heating by Tertiary dykes (northwest Scotland). Org Geochem. 1995;22:165–77. doi: 10.1016/0146-6380(95)90015-2.
[53] Cooper JR, Crelling JC, Rimmer SM, Whittington AG. Coal metamorphism by igneous intrusion in the Raton Basin, CO and NM. Implications for generation of volatiles. Int J Coal Geol. 2007;71:15–27. doi: 10.1016/j.coal.2006.05.007.
[54] Iyer K, Schmid DW. Comment on "Thickness matters: influence of dolerite sills on the thermal maturity of surrounding rocks in a coal bed methane play in Botswana" by Bulguroglu and Milkov (2020). Mar Pet Geol. 2020;115:104247. doi: 10.1016/j.marpetgeo.2020.104247. Forthcoming 2020.
[55] Bulguroglu ME, Milkov AV. Thickness matters: Influence of dolerite sills on the thermal maturity of surrounding rocks in a coal bed methane play in Botswana. Mar Pet Geol. 2020;111:219–29. doi: 10.1016/j.marpetgeo.2019.08.016.
[56] Waples DW. Geochemistry in petroleum exploration. Boston: Int Hum Resour Dev Corporation; 1985. doi: 10.1007/978-94-009-5436-6.

[57] Aarnes I, Podladchikov Y, Svensen H. Devolatilization-induced pressure build-up: Implications for reaction front movement and breccia pipe formation. Geofluids. 2012;12:265–79. doi: 10.1111/j.1468-8123.2012.00368.x.
[58] Saghafi A, Pinetown KL, Grobler PG, van Heerden JHP. CO_2 storage potential of South African coals and gas entrapment enhancement due to igneous intrusions. Int J Coal Geol. 2008;73:74–87. doi: 10.1016/j.coal.2007.05.003.
[59] Shi Q, Qin B, Liang H, Gao Y, Bi Q, Qu B. Effects of igneous intrusions on the structure and spontaneous combustion propensity of coal: a case study of bituminous coal in Daxing Mine, China. Fuel. 2018;216:181–9. doi: 10.1016/j.fuel.2017.12.012.
[60] Curtis ME, Cardott BJ, Sondergeld CH, Rai CS. Development of organic porosity in the Woodford Shale with increasing thermal maturity. Int J Coal Geol. 2012;103:26–31. doi: 10.1016/j.coal.2012.08.004.
[61] Guo H, Jia W, Peng P, Zeng J, He R. Evolution of organic matter and nanometer-scale pores in an artificially matured shale Yanchang Shale. Org Geochem. 2017;105:56–66. doi: 10.1016/j.orggeochem.2017.01.004.
[62] Jarvie DM, Hill RJ, Ruble TE, Pollastro RM. Unconventional shale-gas systems, The Mississippian Barnett Shale of north-central Texas as one model for thermogenic shale-gas assessment. AAPG Bull. 2007;91:475–99. doi: 10.1306/12190606068.
[63] Löhr SC, Baruch ET, Hall PA, Kennedy MJ. Is organic pore development in gas shales influenced by the primary porosity and structure of thermally immature organic matter. Org Geochem. 2015;87:119–32. doi: 10.1016/j.orggeochem.2015.07.010.
[64] Loucks RG, Reed RM, Ruppel SC, Hammes U. Spectrum of pore types and networks in mudrocks and a descriptive classification for matrix-related mudrock pores. AAPG Bull. 2012;96:1071–98. doi: 10.1306/08171111061.
[65] Pommer M, Milliken K. Pore types and pore-size distributions across thermal maturity, Eagle Ford Formation, southern Texas. AAPG Bull. 2015;99:1713–44. doi: 10.1306/03051514151.